Proc. Natl. Acad. Sci. USA
Vol. 93, pp. 377–382, January 1996
Biophysics

Phase separation in aqueous solutions of lens γ-crystallins: Special role of γ_S

(ternary mixture/cataract)

CANWEN LIU, NEER ASHERIE, ALEKSEY LOMAKIN, JAYANTI PANDE, OLUTAYO OGUN, AND GEORGE B. BENEDEK*

Department of Physics, and Center for Materials Sciences and Engineering, Massachusetts Institute of Technology, Cambridge, MA 02139

Contributed by George B. Benedek, September 30, 1995

ABSTRACT **We have studied liquid–liquid phase separation in aqueous ternary solutions of calf lens γ-crystallin proteins. Specifically, we have examined two ternary systems containing γ_S—namely, γ_{IVa} with γ_S in water and γ_{II} with γ_S in water. For each system, the phase-separation temperatures $(T_{ph}(\phi))_\alpha$ as a function of the overall protein volume fraction ϕ at various fixed compositions α (the "cloud-point curves") were measured. For the γ_{IVa}, γ_S, and water ternary solution, a binodal curve composed of pairs of coexisting points, (ϕ^I, α^I) and (ϕ^{II}, α^{II}), at a fixed temperature (20°C) was also determined. We observe that on the cloud-point curve the critical point is at a higher volume fraction than the maximum phase-separation temperature point. We also find that typically the difference in composition between the coexisting phases is at least as significant as the difference in volume fraction. We show that the asymmetric shape of the cloud-point curve is a consequence of this significant composition difference. Our observation that the phase-separation temperature of the mixtures in the high volume fraction region is strongly suppressed suggests that γ_S-crystallin may play an important role in maintaining the transparency of the lens.**

Phase separation of the eye lens cytoplasm has been implicated in cataract formation (1), where opacification of the eye lens results from disturbances in the uniform spatial distribution of the lens proteins (2, 3). The lens proteins primarily involved in phase separation are the γ-crystallins (4), a family of lens-specific monomeric proteins. Previous studies (5–7) have focused on phase separation in binary aqueous solutions of pure, individual members of the calf lens γ-crystallin family. These proteins fall into two groups: the "high-T_c" ($T_c \approx 38$°C) proteins γ_{IIIa} (γ_C) and γ_{IVa} (γ_E) and the "low-T_c" ($T_c \approx 5$°C) proteins γ_{II} (γ_B) and γ_{IIIb} (γ_D). Here T_c is the critical temperature of a binary solution, which is also the maximum phase-separation temperature (T_{ph}) on the coexistence curve in the temperature and volume fraction phase diagram. The critical volume fractions (ϕ_c) of all these γ-crystallins studied are approximately the same ($\phi_c = 0.21 \pm 0.02$) (7).

The lens cell, however, contains multiple protein species (8). Thus it is important to understand the phase-separation behavior of multicomponent aqueous solutions of lens proteins. We have therefore begun a systematic study of the phase-separation properties of protein ternary solutions each consisting of two species of lens proteins in water.

The phase boundary for liquid–liquid phase separation in a ternary solution is a coexistence surface in the three-dimensional temperature (T), overall protein volume fraction [$\phi = (N_A + N_B)\Omega_P/V$], and composition [$\alpha = N_A/(N_A + N_B)$] phase diagram. Here N_A and N_B are the numbers of protein molecules of type A and type B, and V is the total volume of the solution. The effective volume Ω_P of a single protein molecule is assumed to be the same for both species. The coexistence surface $T = T_{ph}(\phi, \alpha)$ separates the one-phase regime ($T > T_{ph}$) from the two-phase regime ($T < T_{ph}$). If one starts with a one-phase sample of fixed volume fraction and composition and lowers the temperatures to below T_{ph}, then two coexisting phases, designated as (ϕ^I, α^I) and (ϕ^{II}, α^{II}), appear. Such coexisting phases are represented by pairs of points at the same temperature on the coexistence surface. The line connecting each pair of coexisting points is called a tie-line. All coexisting points at this temperature constitute the binodal curve. There is a special line on the coexistence surface formed by points representing pairs of coexisting phases infinitely close in both composition and volume fraction. At each point on this line, coexisting phases become indistinguishable. This line is the so-called "critical line," and we will refer to any point on this critical line as a critical point.

We have previously published (9, 10) our experimental and theoretical study of the coexistence surface $T_{ph}(\phi, \alpha)$ for aqueous ternary solutions consisting of various combinations of the proteins γ_{IIIa}, γ_{IVa}, γ_{II}, and γ_{IIIb}. For such ternary solutions, the coexistence surface has a simple feature: the constant α sections $(T_{ph}(\phi))_\alpha$ of the coexistence surface (the "cloud-point curves") retain their shape and can be obtained by a vertical displacement (along the T axis) of the coexistence curves of the corresponding binary solutions. In addition, the critical points of the ternary mixture at all compositions α remain at the same concentration as the critical volume fractions of the binary solutions. We have found that both of these features result from the fact that the interaction energies among the γ-crystallins mentioned above differ by less than k_BT, where k_B is the Boltzmann constant. Such proteins may be designated as "similar proteins."

In this paper we examine protein ternary solutions that include an important member of the γ-crystallin family, γ_S-crystallin. γ_S is a monomeric protein of a molecular mass and radius about the same as those of the other γ-crystallins—i.e., 21 kDa and 24 Å, respectively. Examination of binary aqueous solutions of pure γ_S-crystallin showed that, under the conditions used to study other pure γ-crystallins, γ_S solutions do not phase separate at temperatures as low as −10°C. In addition, our separate studies show that γ_S suppresses the aggregation of γ_{II}-crystallin and γ_{IVa}-crystallin (C.L., J.P., A.L., O.O., and G.B.B., unpublished data). In both bovine and human lenses, the synthesis of γ_S-crystallin increases with age. In contrast, other γ-crystallins are mainly expressed prenatally, and their syntheses decrease progressively during the development of lens (11–14). These properties of γ_S-crystallin lead us to hypothesize that γ_S may play an important role in maintaining the transparency of the lens.

We therefore undertook an investigation of the effect of γ_S on the phase-separation temperature of other lens proteins in mixtures where increasing amounts of γ_S are present. We present here our studies of two ternary solutions composed of

The publication costs of this article were defrayed in part by page charge payment. This article must therefore be hereby marked "*advertisement*" in accordance with 18 U.S.C. §1734 solely to indicate this fact.

Abbreviations: DTT, dithiothreitol; T_c, critical temperature; T_{ph}, phase-separation temperature.

*To whom reprint requests should be addressed.

a high-T_c protein γ_{IVa} and γ_S in water and a low-T_c protein γ_{II} and γ_S in water. In each of the two ternary systems studied, we designate γ_S as protein B, and solvent water as W. The other protein in the mixture, γ_{IVa} or γ_{II}, is denoted as protein A.

We have found that γ_S has a profound effect on the phase-separation properties of the ternary solutions. As the proportion of γ_S-crystallin in the solution increases (and α consequently decreases), the cloud-point curve, $(T_{ph}(\phi))_\alpha$, becomes increasingly asymmetric about the critical point. The critical point itself shifts with decreasing α to higher protein volume fraction, while the maximum phase-separation temperature point moves to lower volume fractions. As a result, increasing amounts of γ_S strongly lower the phase-separation temperatures of the mixtures at higher protein volume fractions. This is consistent with the view that the presence of γ_S in the lens helps maintain its transparency.

We designate the protein pairs γ_{IVa}/γ_S and γ_{II}/γ_S, which exhibit the above features, as "dissimilar proteins." For a full analysis of the phase-separation properties of ternary solutions of dissimilar proteins, one needs to construct the Gibbs free energy and apply the equilibrium conditions for the coexistence of two phases. Such analysis falls beyond the scope of this work and will be the subject of a future publication. Here, we present general considerations which demonstrate that the asymmetric features of the cloud-point curves are the result of the significant composition differences between the coexisting phases near the critical point.

MATERIALS AND METHODS

Preparation of Pure γ-Crystallin Solutions. The native γ-crystallin fractions γ_S, γ_{II}, γ_{III}, and γ_{IV} were isolated from calf eye lens as described earlier (5, 15). The γ_S–γ_{II} fraction thus obtained was run on a second SP-Sephadex C-50 column, followed by elution on a QAE-Sephadex column with a 2-liter linear gradient of 0–50 mM NaCl in 25 mM ethanolamine (pH 9.4). Native γ_{IV}-crystallin obtained by cation-exchange chromatography was further purified into γ_{IVa} and γ_{IVb} (7). The single protein species were found to be 99% pure by cation-exchange HPLC (16) and isoelectric focusing.

The purified crystallin fractions were dialyzed exhaustively into 100 mM (pH 7.1) sodium phosphate buffer (ionic strength of 240 mM) containing 0.02% sodium azide. For experiments involving γ_{II}-crystallin, an additional 20 mM dithiothreitol (DTT) was added to the buffer to suppress aggregation (17). The concentrations of the pure protein samples were determined by UV absorption at 280 nm. The extinction coefficients $\varepsilon_{280}^{0.1\%,\ 1cm}$ for γ_{IVa}, γ_{II}, and γ_S are 2.25, 2.18 (7), and 2.0, respectively.

Protein ternary solutions were prepared as explained (9, 10). The overall protein volume fraction ϕ was obtained from the total protein concentration C (in mg/ml) by using the specific volume $\bar{v}$ with $\phi = \bar{v}C$. We assume that the specific volumes for all γ-crystallins are approximately the same as that of γ_{II}-crystallin [$\bar{v} = 0.71$ cm^3/g (6)]. The compositions α of ternary solutions were determined by HPLC. Precautions were taken to obtain aggregate-free and crystal-free homogeneous protein solutions (7, 10, 18).

The experimental methods used to obtain cloud-point curves and binodal curves have been described in detail elsewhere (9, 10). Below we discuss briefly the determination of the phase-separation temperature T_{ph} by the cloud-point method and show how this method allows us to identify the critical points.

The Cloud-Point Method and the Determination of the Critical Points. The phase-separation temperature T_{ph} for a ternary solution of volume fraction ϕ and composition α was determined by the cloud-point method (5, 10, 19) as follows. The solution, which was contained in a test tube 4 mm in diameter, was placed in a water cell connected to a circulating water bath. The actual temperature of the sample was measured (with a precision of 0.1°C) by placing a thermocouple close to the test tube containing the sample. A 0.4-mW He-Ne laser was focused on the sample, and the transmitted light intensity was received by a photodiode. The transmitted light intensity, the temperature of the sample, and the temperature setting of the water bath were all recorded by a computer. The sample was initially maintained in the single-phase state, and the initial value of the transmitted light intensity was registered. The temperature of the water bath was then lowered at a rate of 0.005°C/sec. When the temperature of the sample reached a certain value, domains of the protein-rich and protein-poor phases began to form. As a result, strong light scattering occurred due to inhomogeneities in the refractive index of the solution (2), and the transmitted light intensity dropped. The temperature of the water bath was then raised until the transmitted intensity recovered its initial value (i.e., the sample became transparent again).

Fig. 1 *A–C* shows the transmitted intensity–temperature profile for an off-critical [($\phi \ll \phi_c$ or $\phi \gg \phi_c$; Fig. 1*A*), near-critical ($\phi < \phi_c$ or $\phi > \phi_c$; Fig. 1*B*), and critical ($\phi = \phi_c$; Fig. 1*C*)] solution. Fig. 1*A* shows that for an off-critical solution there is a hysteresis in the transmitted intensity as a function of temperature—that is, clouding occurs at a lower temperature (T_{cloud}) than clarification ($T_{clarify}$). This hysteresis in intensity is due to the fact that phase separation for an off-critical solution occurs via nucleation and droplet growth (20), and the system has to overcome a nucleation energy barrier to induce the formation of new phases. In Fig. 1*A*, I_{ref} is the initial transmitted light intensity, which we took as a reference intensity. $I_{50\%}$ is the intensity at 50% of the reference value. We took the temperature at which the transmitted light intensity drops to $I_{50\%}$ as the clouding temperature (T_{cloud}).

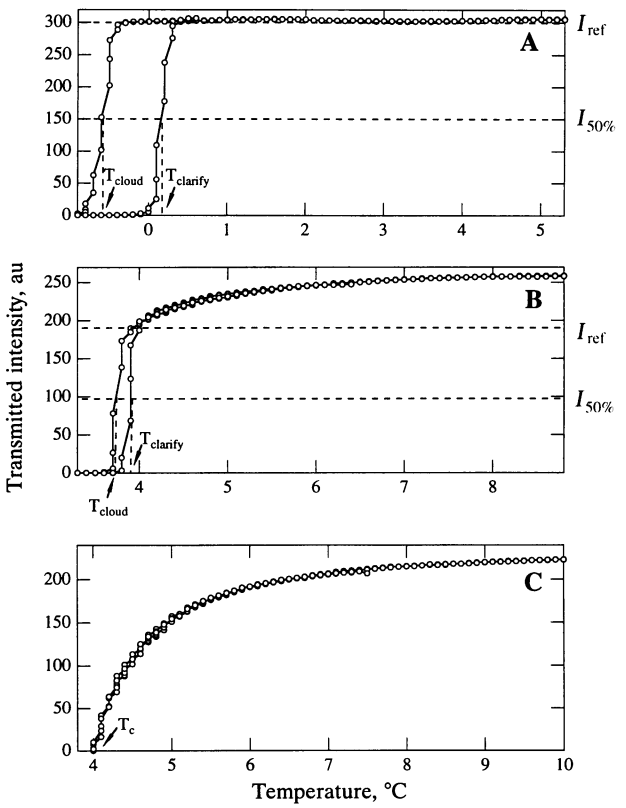

FIG. 1. The transmitted light intensity versus temperature profiles for γ_{IIIb}/water binary solutions at three different concentrations. (*A*) $\phi \ll \phi_c$ or $\phi \gg \phi_c$. (*B*) $\phi < \phi_c$ or $\phi > \phi_c$. (*C*) $\phi = \phi_c$. au, Arbitrary units; $I_{50\%}$, intensity at 50% of the reference value; I_{ref}, reference transmitted intensity.

Similarly, we took the temperature at which the transmitted intensity returns to $I_{50\%}$ as the clarification temperature ($T_{clarify}$). The T_{ph} of the solution is defined as $T_{ph} = (T_{cloud} + T_{clarify})/2$, and the uncertainty in T_{ph} is $\Delta T_{ph} = (T_{clarify} - T_{cloud})/2$. For a near-critical solution (Fig. 1*B*), there is a gradual decrease in the transmitted light intensity followed by a rapid drop. This gradual decrease before the phase transition occurs is related to the critical fluctuations in a solution close to the critical concentration. The hysteresis in Fig. 1*B* becomes narrower—i.e., ΔT_{ph} becomes smaller, compared to that for an off-critical solution in Fig. 1*A*, due to the fact that the nucleation energy is lower. In this case, I_{ref} was taken to be the transmitted light intensity at which the hysteresis starts. For a critical solution (Fig. 1*C*), the transmitted intensity drops gradually. When the temperature of the solution is raised, the intensity traces back to its original value without any lag. As shown in Fig. 1*C*, there is no hysteresis for a critical solution. This gradual change in the transmitted intensity is a consequence of the continuous growth of the concentration fluctuations in the solution as the critical temperature is approached from above. We have used this intensity profile to identify the critical point on the cloud-point curve. The temperature at which the transmitted intensity disappears was taken as the critical temperature T_c of the solution.

RESULTS

The γ_{IVa}, γ_S, and Water Ternary Solutions. *Cloud-point curves.* In Fig. 2 we present our measurements of the constant α sections (cloud-point curves), $(T_{ph}(\phi))_\alpha$, of the coexistence surface of γ_{IVa}, γ_S, and water ternary solutions at α = 0.17, 0.34, 0.43, 0.61, 0.68, 0.91, and 1.0. The data corresponding to α = 1.0 (γ_{IVa}) were taken from Broide *et al.* (7). The experimentally determined critical points at several compositions are shown as squares containing an X. Notice that for the γ_{IVa}/water binary solution (α = 1.0), the critical point occurs at the maximum phase-separation temperature point on the coexistence curve. However, as the amount of γ_S in the solution increases (i.e., α decreases), the cloud-point curves, $(T_{ph}(\phi))_\alpha$, of the ternary mixture become increasingly asymmetric, with the critical points shifting to higher protein volume fractions. At the same time, the maxima shift to lower volume fractions. For ternary mixtures with $\alpha \leq 0.43$, we did not observe the transmitted intensity–temperature profile for critical solutions as shown in Fig. 1*C*, even with the most concentrated samples. We thus conclude that the critical volume fractions, ϕ_c, for these ternary mixtures are greater than the highest volume fractions studied at each α.

The binodal curve. In Fig. 3 we present our experimental data (solid symbols) on coexisting values (ϕ^I, α^I) and (ϕ^{II}, α^{II}) found upon quenching ternary mixtures below the coexistence surface to a temperature T = 293.2 K (20°C) at several initial overall protein volume fractions and compositions (ϕ^0, α^0) = (0.15, 0.57), (0.12, 0.68), (0.06, 0.91), and (0.12, 1.0). The pairs of points representing the coexisting phases (ϕ^I, α^I) and (ϕ^{II}, α^{II}) are connected by straight lines (tie-lines). Open diamonds and crossed square in Fig. 3 represent the equilibrium points and the critical point (ϕ_c, α_c, T_c) = (0.31, 0.68, 293.2 K) on the binodal curve, respectively, deduced from the cloud-point curve data as shown in Fig. 2. The solid curve is an eye guide for the binodal curve. The dashed line represents the tangent to the binodal curve or the slope of tie-line at the critical point and will be discussed later. One important feature of Fig. 3 is the significant difference in the compositions of coexisting phases near the critical point, as reflected in the large slopes of the tie-lines.

The γ_{II}, γ_S, and Water Ternary Solutions. *Cloud-point curves.* In Fig. 4 we present our measurements of the cloud-point curves of γ_{II}, γ_S, and water ternary solutions (in 100 mM phosphate buffer with 20 mM DTT) at α = 0.70, 0.86, 0.91, and 1.0. We found that the presence of 20 mM DTT lowers the T_{ph} of pure γ_{II} solution by ≈2°C (17). Thus the data corresponding to the aqueous γ_{II} binary solution (α = 1.0), taken from Broide *et al.* (7) [which was modified from Thomson *et al.* (5)], were shifted by −2 K. Fig. 4 shows that the cloud-point curves of the γ_{II}, γ_S, and water ternary solutions are also asymmetric. However, the critical volume fractions of the ternary mixtures move only slightly to higher volume fractions as α decreases. This is in contrast to the case of γ_{IVa}, γ_S, and water ternary solutions, where we have observed a large shift of the critical volume fractions of the mixture. On the other hand, for the γ_{II}, γ_S, and water ternary solutions, the maxima on the cloud-point curves show stronger shifts to lower protein volume fractions than those of the γ_{IVa}, γ_S, and water ternary solutions. The asymmetric shape of cloud-point curves is also observed in

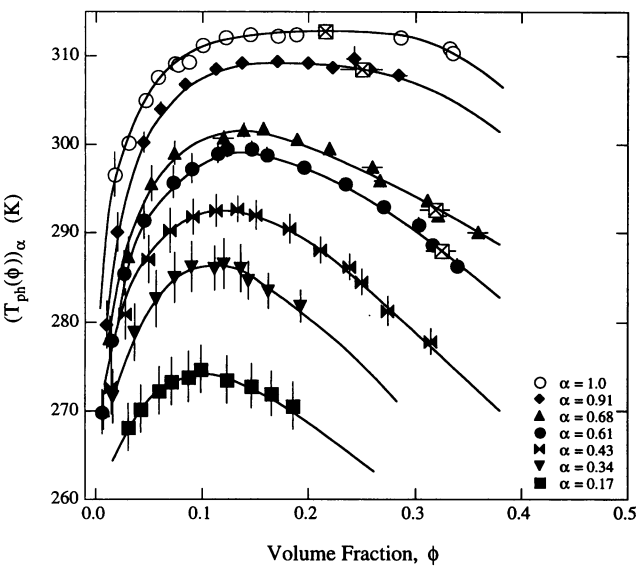

FIG. 2. The constant α sections (cloud-point curves) of the coexistence surface of aqueous ternary solutions of purified calf γ-crystallins γ_{IVa} and γ_S at fixed compositions. The data for α = 1.0 (γ_{IVa}) were taken from Broide *et al.* (7). ⊠, Measured critical points of the mixtures at several compositions. The solid curves are eye guides to show trends in the data. The solution conditions were (pH 7.1) 100 mM phosphate buffer (ionic strength, 240 mM).

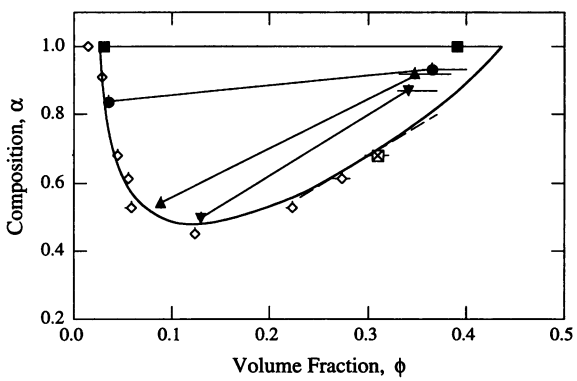

FIG. 3. Pairs of points (solid symbols) connected by straight lines (i.e., tie-lines) represent the two coexisting phases at T = 293.2 K for aqueous ternary solutions of γ_{IVa} and γ_S at various initial solution volume fractions and compositions (ϕ^0, α^0) = (0.15, 0.57) (▼), (0.12, 0.68) (▲), (0.06, 0.91) (●), and (0.12, 1.0) (■). The critical point (⊠) and the equilibrium data points (◇) are deduced from the cloud-point curve data in Fig. 2. The solid curve is an eye guide for the binodal curve. The slope of the tie-line (dashed line) at the critical point is drawn as discussed in the text.

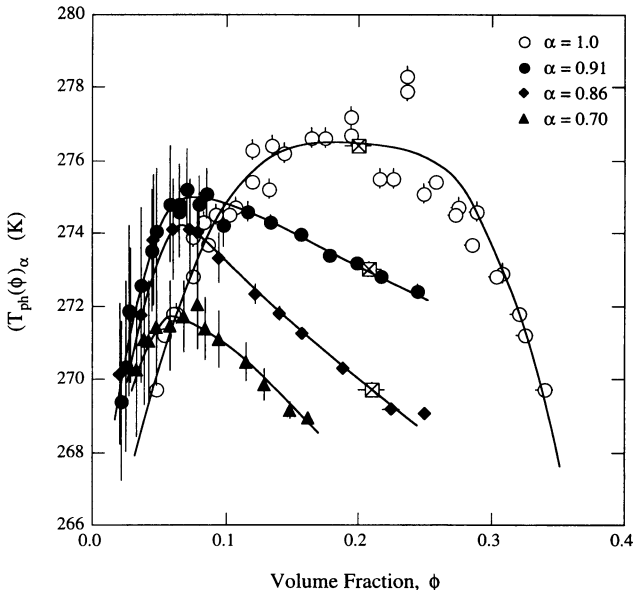

FIG. 4. The constant α sections (cloud-point curves) of the coexistence surface of γ_{II}, γ_S, and water ternary solutions at fixed compositions α. The solution conditions were (pH 7.1) 100 mM phosphate buffer, ionic strength of 240 mM, in the presence of 20 mM DTT. The data for $\alpha = 1.0$ (γ_{II}) were taken from Broide *et al.* (7) [modified from Thomson *et al.* (5)] and shifted by -2 K to account for the effect of 20 mM DTT. ⊠, Experimentally measured critical points. The solid curves are eye guides to show trends in the data.

polydisperse polymer solutions (21, 22), aqueous protein/polysaccharide systems (23), and aqueous ternary solutions of γ-crystallins and lysozyme (10).

DISCUSSION

Physical insight into the phenomena described above can be achieved using geometrical considerations. It follows from the general properties of surfaces that for any point (ϕ, α, T) on the coexistence surface $T = T_{ph}(\phi, \alpha)$, the partial derivatives satisfy a relationship: $(\partial T/\partial\phi)_\alpha(\partial\phi/\partial\alpha)_T(\partial\alpha/\partial T)_\phi = -1$. On the temperature, volume fraction, and composition three-dimensional phase diagram, $(\partial T/\partial\phi)_\alpha$, $(\partial T/\partial\alpha)_\phi$, and $(\partial\alpha/\partial\phi)_T$ are, respectively, the tangents of the constant α section (cloud-point curve), constant ϕ section, and constant T section (binodal curve) of the coexistence surface at (ϕ, α, T). This general relationship among the three variables enables one to deduce the tangent of one section of the coexistence surface when those of the other two are known. It becomes particularly useful when applied to a critical point (as denoted by a superscript c) where the tangent $(\partial\alpha/\partial\phi)_T^c$ becomes the limiting slope of the tie-lines at this critical point on the binodal curve. Thus $(\partial\alpha/\partial\phi)_T^c$ is a physically important quantity, which reflects the composition difference in the coexisting phases. Rewriting the above relationship at a critical point we have

$$\left(\frac{\partial T}{\partial\phi}\right)_\alpha^c = -\left(\frac{\partial T}{\partial\alpha}\right)_\phi^c\left(\frac{\partial\alpha}{\partial\phi}\right)_T^c. \qquad [1]$$

If $(\partial T/\partial\phi)_\alpha^c \neq 0$, then the critical point on the cloud-point curve is not an extremum, and thus the curve is asymmetric. In particular, if $(\partial T/\partial\phi)_\alpha^c < 0$, the critical point on the cloud-point curve is at a higher volume fraction than the maximum. This is the case for the ternary solutions we have studied. Thus Eq. **1** shows how the asymmetry of the cloud-point curves is related to the composition difference in the coexisting phases near the critical point.

The use of Eq. **1** is illustrated explicitly in Fig. 5 *A–C*, where we show schematically the phase diagrams for the ternary solutions of γ_{IVa} and γ_S. In this figure we present, respectively, the constant T section (Fig. 5*A*), constant ϕ section (Fig. 5*B*), and constant α section (Fig. 5*C*) of the coexistence surface through the critical point (ϕ_c, α_c) corresponding to the temperature T (= 293.2 K) of the experimental binodal curve. In Fig. 5*A* the tie-lines and the slope of tie-line at the critical point are shown as dashed lines. The form of the corresponding constant $\phi = \phi_c$ section (Fig. 5*B*) is deduced from the cloud-point curve data in Fig. 2. We found that $(T_{ph}(\alpha))_\phi$ is approximately a linear function of α near the critical point. Fig. 5*C* shows the corresponding cloud-point curve at $\alpha = \alpha_c$. We see that the slope of the tie-lines near the critical point is large, $(\partial\alpha/\partial\phi)_T^c > 0$ (Fig. 5*A*), and that the slope of the constant ϕ section of the coexistence surface is positive, $(\partial T/\partial\alpha)_\phi^c > 0$ (Fig. 5*B*). Therefore, according to Eq. **1**, the slope of the cloud-point curve at the critical point should have a large negative value, $(\partial T/\partial\phi)_\alpha^c < 0$ (Fig. 5*C*). This connects the asymmetric shape of the cloud-point curve and the shift of the critical point from the maximum with the large slope of the tie-lines near the critical point.

The observed features of the coexistence surface of γ_{II}, γ_S, and water ternary solutions can be explained similarly. Fig. 5 *D–F* shows schematically the phase diagrams for this ternary system through a critical point (ϕ_c, α_c) corresponding to the temperature T (= 269.6 K). Here we deduced the shapes of both the binodal curve (Fig. 5*D*) and the constant ϕ section (Fig. 5*E*) from the cloud-point curve data in Fig. 4. We do not have information on the positions of coexisting points (tie-lines) on the binodal curve. In this ternary mixture, we see again that the large slope of tie-line near the critical point, $(\partial\alpha/\partial\phi)_T^c > 0$ (Fig. 5*D*), and the positive slope of the constant ϕ section, $(\partial T/\partial\alpha)_\phi^c > 0$ (Fig. 5*E*), are connected to a negative $(\partial T/\partial\phi)_\alpha^c$. This is consistent with the observed asymmetric cloud-point curve (Fig. 5*F*).

It is interesting to compare the phase-separation properties of ternary solutions containing γ_S with those of ternary solutions of similar proteins that we have analyzed in detail previously (9, 10). The qualitative features of the coexistence surface in this case are shown in Fig. 5 *G–I*. For ternary solutions of similar proteins, the slope of tie-line $(\partial\alpha/\partial\phi)_T^c$ near the critical point is very small (Fig. 5*G*). The critical line stays

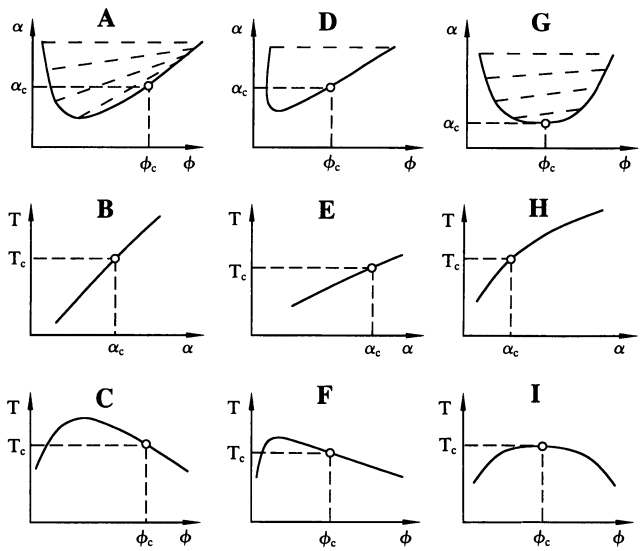

FIG. 5. The schematic phase diagrams for the constant T section (binodal curve), constant ϕ section, and constant α section (cloud-point curve) of the coexistence surfaces of ternary solutions of γ_{IVa} and γ_S (*A–C*), γ_{II} and γ_S (*D–F*), and γ_{IIIa} and γ_{IIIb} (*H–I*). The critical points are shown as open circles. The tie-lines are shown as dashed lines.

Table 1. The numerical values of $(\partial T/\partial\phi)^c_\alpha$, $(\partial T/\partial\alpha)^c_\phi$, and $(\partial\alpha/\partial\phi)^c_T$

Ternary solution	Critical point (ϕ_c, α_c, T)	Experimental $(\partial T/\partial\phi)^c_\alpha$, K	Experimental $(\partial T/\partial\alpha)^c_\phi$, K	Calculated $(\partial\alpha/\partial\phi)^c_T$
$\gamma_{IVa} + \gamma_s$	(0.31, 0.68, 293.2 K)	-79.0 ± 6.0	54.3 ± 5.5	1.5 ± 0.2
$\gamma_{II} + \gamma_s$	(0.21, 0.86, 269.6 K)	-28.5 ± 2.6	23.5 ± 6.1	1.2 ± 0.3
$\gamma_{IIIa} + \gamma_{IIIb}$	(0.21, 0.30, 293.2 K)	-4.2 ± 1.0	41.1 ± 1.1	0.10 ± 0.02

at constant $\phi = \phi_c$, and $(T_{ph}(\alpha))_\phi$ is approximately a quadratic function of α at this fixed ϕ (Fig. 5*H*). The cloud-point curve is nearly symmetric with the critical point being approximately at its maximum (Fig. 5*I*). Indeed, the very small slope of the tie-line near the critical point (Fig. 5*G*) and the finite slope of the constant ϕ section (Fig. 5*H*) are consistent with the small slope of the cloud-point curve at the critical point (Fig. 5*I*) as expected from Eq. **1**.

From the general considerations presented above, we see that the shape of the cloud-point curves, $(T_{ph}(\phi))_\alpha$, is closely related to the composition differences in the coexisting phases near the critical point, as reflected in the slope of tie-line $(\partial\alpha/\partial\phi)^c_T$. We therefore conclude that the quantity $(\partial\alpha/\partial\phi)^c_T$ is of primary importance in determining the general features of the coexistence surface.

The exact relationship given by Eq. **1** is also useful in determining a reliable value of $(\partial\alpha/\partial\phi)^c_T$, since the other two quantities $(\partial T/\partial\phi)^c_\alpha$ and $(\partial T/\partial\alpha)^c_\phi$ can be determined relatively accurately from the cloud-point curves and the constant ϕ sections of the coexistence surface. Experimentally it is very difficult to measure $(\partial\alpha/\partial\phi)^c_T$ directly (i.e., to measure the slope of tie-lines in the immediate vicinity of the critical point), since the phase-separation dynamics near the critical region is extremely slow. One of the indirect ways to obtain $(\partial\alpha/\partial\phi)^c_T$ is to deduce it from the binodal curve. The reconstruction of the binodal curve both from the coexisting points (ϕ^I, α^I) and (ϕ^{II}, α^{II}) and from the interpolation of data points on the cloud-point curves and the constant ϕ sections of the coexistence surface involves several difficulties. These include the poor accuracy in determining equilibrium values (ϕ^I, α^I) and (ϕ^{II}, α^{II}) and the difficulty in preparing highly concentrated samples ($\phi > \phi_c$) for measurements of the cloud-point curves and constant ϕ sections (10). Thus the differential relationship in Eq. **1** provides a convenient and relatively accurate means to determine the value of $(\partial\alpha/\partial\phi)^c_T$, as we demonstrate below for the ternary solutions we studied.

In Table 1 we list the numerical values of the various derivatives in Eq. **1**. We present in columns 1 and 2 the various ternary systems and the corresponding critical point (ϕ_c, α_c) at certain temperatures T. Columns 3 and 4 list the values of $(\partial T/\partial\phi)^c_\alpha$ and $(\partial T/\partial\alpha)^c_\phi$, respectively, as determined from the cloud-point curves of our ternary solutions. These quantities have been obtained by two-dimensional linear interpolation of the data in the vicinity of the critical point listed in column 2. In the last column, we give the values of $(\partial\alpha/\partial\phi)^c_T$ calculated from Eq. **1**, using the values of $(\partial T/\partial\phi)^c_\alpha$ and $(\partial T/\partial\alpha)^c_\phi$ in columns 3 and 4. Note that in Fig. 3 the tangent at the critical point (shown as a dashed line) has been drawn using the value of $(\partial\alpha/\partial\phi)^c_T = 1.5 \pm 0.2$ from Table 1. For comparison, we also include in row 3 the corresponding values for the similar proteins γ_{IIIa} and γ_{IIIb} from refs. 9 and 10.

The results for $(\partial\alpha/\partial\phi)^c_T$ in the last column of Table 1 suggest a classification scheme for characterizing ternary solutions. We know that when $(\partial\alpha/\partial\phi)^c_T$ is sufficiently small the proteins may be considered as similar (9, 10). From our data we see that $(\partial\alpha/\partial\phi)^c_T$ is about 10 times larger for the ternary solutions that contained γ_s-crystallin than that for the similar proteins γ_{IIIa} and γ_{IIIb}. This leads us to classify the protein pairs γ_{IVa}/γ_s and γ_{II}/γ_s as dissimilar. It may be shown that the large value of $(\partial\alpha/\partial\phi)^c_T$ is a consequence of a significant difference in the protein interactions. Specifically, in a ternary solution of γ_s with another γ-crystallin, the interaction energy of two γ_s proteins or the interaction energy of γ_s with the other γ-crystallin must be different, by k_BT or more, from the interaction energy between two of the other γ-crystallins. This is in contrast to the case of similar proteins. Thus the thermodynamic properties of γ_s set it apart from the other members of the γ-crystallin family. This finding supports the view that γ_s may play a special role in maintaining the transparency of the lens.

SUMMARY AND CONCLUSIONS

We have presented our measurements of the coexistence surfaces of aqueous ternary solutions for two pairs of dissimilar proteins: γ_{IVa}/γ_s and γ_{II}/γ_s. We have observed that for these ternary systems, the composition difference in the coexisting phases near the critical point is large. In addition, the cloud-point curve is asymmetric and the critical point is at higher volume fraction than that of the maximum phase-separation temperature point. These phase-separation properties differ significantly from those of the ternary solutions of similar proteins that we have studied before. We have shown generally that for ternary solutions of dissimilar proteins, the asymmetric shape of the cloud-point curve is a result of the significant composition difference between the coexisting phases, as reflected in the large slope of tie-line $(\partial\alpha/\partial\phi)^c_T$ near the critical point. We have demonstrated that the differential relationship between T, ϕ, and α provides a reliable value for the important quantity $(\partial\alpha/\partial\phi)^c_T$. We have also shown that the magnitude of this quantity allows us to classify different ternary systems. The experimental evidence that the presence of γ_s in the concentrated solutions of other γ-crystallins lowers the phase-separation temperatures significantly and the fact that γ_s also suppresses the aggregation of γ-crystallin solutions support the view that this protein may play an important role in maintaining the transparency of the lens.

We thank Professor Felix Villars and Dr. George Thurston for valuable suggestions and critical comments. This work was supported by Grants EY05127 (G.B.B.) and EY10535 (J.P.) from the National Eye Institute of the National Institutes of Health.

1. Benedek, G. B. (1984) *Human Cataract Formation*, Ciba Foundation Symposium 106 (Pitman, London), pp. 237–247.
2. Benedek, G. B. (1971) *Appl. Optics* **10**, 459–473.
3. Tardieu, A., Veretout, F., Krop, B. & Slingsby, C. (1992) *Eur. Biophys. J.* **21**, 1–12.
4. Siezen, R. J., Fisch, M. R., Slingsby, C. & Benedek, G. B. (1985) *Proc. Natl. Acad. Sci. USA* **82**, 1701–1705.
5. Thomson, J. A., Schurtenberger, P., Thurston, G. M. & Benedek, G. B. (1987) *Proc. Natl. Acad. Sci. USA* **84**, 7079–7083.
6. Schurtenberger, P., Chamberlin, R. A., Thurston, G. M., Thomson, J. A. & Benedek, G. B. (1989) *Phys. Rev. Lett.* **63**, 2064–2067.
7. Broide, M. L., Berland, C. R., Pande, J., Ogun, O. O. & Benedek, G. B. (1991) *Proc. Natl. Acad. Sci. USA* **88**, 5660–5664.
8. Wistow, G. J. & Piatigorsky, J. (1988) *Annu. Rev. Biochem.* **57**, 479–504.
9. Liu, C., Lomakin, A., Thurston, G. M., Hayden, D., Pande, A., Pande, J., Ogun, O., Asherie, N. & Benedek, G. B. (1995) *J. Phys. Chem.* **99**, 454–461.
10. Liu, C. (1995), Ph.D. thesis (Massachusetts Institute of Technology, Cambridge).
11. van Dam, A. F. (1966) *Exp. Eye Res.* **8**, 255–266.

12. Croft, L. R. (1973) *The Human Lens in Relation to Cataract*, Ciba Foundation Symposium 19 (Elsevier, Amsterdam), pp. 207–224.
13. Zigler, J. S., Jr., & Horwitz, J. (1981) *Exp. Eye Res.* **32,** 21–30.
14. Nagineni, C. N. & Bhat, S. P. (1992) *Exp. Eye Res.* **54,** 193–200.
15. Bjork, I. (1964) *Exp. Eye Res.* **3,** 254–261.
16. Siezen, R. J., Kaplan, E. D. & Anello, R. D. (1985) *Biochem. Biophys. Res. Commun.* **127,** 153–160.
17. Pande, J., Lomakin, A., Fine, B., Ogun, O., Sokolinski, I. & Benedek, G. (1995) *Proc. Natl. Acad. Sci. USA* **92,** 1067–1071.
18. Berland, C. R., Thurston, G. M., Kondo, M., Broide, M. L., Pande, J., Ogun, O. & Benedek, G. B. (1992) *Proc. Natl. Acad. Sci. USA* **89,** 1214–1218.
19. Taratuta, V. G., Holschbach, A., Thurston, G. T., Blankschtein, D. & Benedek, G. B. (1990) *J. Phys. Chem.* **94,** 2140–2144.
20. Lifshitz, I. M. & Slyozov, V. V. (1961) *J. Phys. Chem. Solids* **19,** 35–50.
21. Kuwahara, N., Fenby, D. V., Tamsky, M. & Chu, B. (1971) *J. Chem. Phys.* **55,** 1140–1148.
22. Kamide, K. (1990) *Thermodynamics of Polymer Solutions: Phase Equilibria and Critical Phenomena* (Elsevier, New York).
23. Antonov, Yu.A., Grinberg, V.Ya. & Tolstoguzov, V. B. (1977) *Coll. Poly. Sci.* **255,** 937–947.